



HAL
open science

Assessing the precision in loading estimates by geodetic techniques in Southern Europe

Pierre Valty, Olivier de Viron, Isabelle Panet, Michel van Camp, Juliette Legrand

► **To cite this version:**

Pierre Valty, Olivier de Viron, Isabelle Panet, Michel van Camp, Juliette Legrand. Assessing the precision in loading estimates by geodetic techniques in Southern Europe. *Geophysical Journal International*, 2013, 194, pp.1441-1454. 10.1093/gji/ggt173 . insu-03581769

HAL Id: insu-03581769

<https://insu.hal.science/insu-03581769>

Submitted on 21 Feb 2022

HAL is a multi-disciplinary open access archive for the deposit and dissemination of scientific research documents, whether they are published or not. The documents may come from teaching and research institutions in France or abroad, or from public or private research centers.

L'archive ouverte pluridisciplinaire **HAL**, est destinée au dépôt et à la diffusion de documents scientifiques de niveau recherche, publiés ou non, émanant des établissements d'enseignement et de recherche français ou étrangers, des laboratoires publics ou privés.



Distributed under a Creative Commons Attribution 4.0 International License

Assessing the precision in loading estimates by geodetic techniques in Southern Europe

Pierre Valty,¹ Olivier de Viron,² Isabelle Panet,^{1,2} Michel Van Camp³
and Juliette Legrand³

¹*Institut National de l'Information Géographique et Forestière/Laboratoire de Recherche en Géodésie, Université Paris-Diderot, bâtiment Lamarck, case 7011, 35 rue Hélène Brion, 75013 Paris, France. E-mail: pierre.valty@ign.fr*

²*Institut de Physique du Globe de Paris (IPGP, Sorbonne Paris-Cité, UMR 7154, CNRS, Université Paris-Diderot), bâtiment Lamarck, Case 7011, 35 rue Hélène Brion, 75013 Paris, France*

³*Observatoire Royal de Belgique, 3 avenue Circulaire, 1180 Bruxelles, Belgium*

Accepted 2013 April 24. Received 2013 April 24; in original form 2012 July 27

SUMMARY

This paper investigates the precision of the estimation of geophysical fluid load deformation computed from GRACE space gravity, GPS vertical displacement and geophysical fluids models [Global Circulation Models (GCMs) for ocean, atmosphere and hydrology], using the three-cornered hat method. This method allows the estimation of the variance of the errors of each technique, when the same quantity is monitored by three instruments with independent errors. Applied on a network of stations, several points of view can be considered: the technique level (in order to determine the error of each technique: GRACE, GPS and GCMs), the solution level (allowing to compare the precision of the same technique when different strategies/models are used), and the station level (in order to emphasize local anomalies and geographical patterns). In particular, our results show a precision of the loading vertical displacement at the level of 1 mm when using GRACE or the fluid models, and of 2 mm using GPS. We do not find significant differences between the precision of different solutions of the same techniques, even when there are strong differences in the data processing.

Key words: Time-series analysis; Space geodetic surveys; Time variable gravity; Global change from geodesy; Europe.

1 INTRODUCTION

Since 2002, the GRACE satellite mission has been measuring the temporal variations of the Earth's gravity field, reflecting the mass redistributions associated with the dynamics of the Earth and its climate system, with an optimal sensitivity to the global water cycle (Tapley *et al.* 2004). Results from GRACE have opened the way to the use of space gravimetry for monitoring water resources and improving hydrological models (Ramillien *et al.* 2005; Güntner *et al.* 2007; Rodell *et al.* 2007; Schmidt *et al.* 2008; Syed *et al.* 2008; Famiglietti *et al.* 2011), as predicted by Wahr *et al.* (1998). The availability of various geoid models however raised the question of understanding to which extent one of the GRACE solutions would be more suited than others for this purpose, stressing the importance of the quantitative assessment of the precision of these different solutions. Beyond the propagation of formal errors as done by Wahr *et al.* (2006), precision estimates are based on intercomparisons of the different GRACE geoid solutions (de Viron *et al.* 2008; Tesmer *et al.* 2011) or comparisons with *in situ* measurements (Chambers 2006; Swenson *et al.* 2006).

In addition to the gravity changes, water mass redistribution also causes the Earth's surface to deform, impacting the time-series

of displacements. Various studies have investigated the consistency between deformation measured by GPS and modelled from GRACE models (Blewitt *et al.* 2001; Blewitt & Clarke 2003; van Dam *et al.* 2007), and more recent studies have shown that this consistency improves with the quality of the GPS data processing (Tregoning *et al.* 2009; Tesmer *et al.* 2011). The agreement between GPS and GRACE has been demonstrated on the annual cycle while much remains to be done at interannual timescale.

Here, we assess the precision of the load vertical deformation as measured by GPS, and as computed from the GRACE time variable gravity and from the climatic Global Circulation Models (GCMs), with emphasis on the interannual timescale. Quantitatively comparing the GRACE geoid time variations with time-series of GNSS surface displacements and model water loads is not straightforward, because GRACE and GNSS sense the effect of the water displacement through their own transfer function, and because observations and models have different spatial and spectral properties. GRACE provides geoid models, GCMs provide mass distribution, and GPS data are surface displacement. Nevertheless, everything can be converted into the same physical observable, in our case the vertical displacement, using the elastogravity theory of the Earth deformation under surface load (Farrell 1972). The space resolution is

different for the three data sets; nevertheless the vertical surface displacements transfer function emphasizes the load signal of medium to large space scale, that is, at a spatial resolution close to that of GRACE. The effective spatial resolution of the displacements associated to the signal contained in the models is close to that of GRACE. Note that we used the vertical displacement only, because the horizontal displacements associated to large and medium scale load are generally much smaller, and, over all, because they are not significantly consistent with the GPS ones on a large number of stations. This has already been shown by several authors, see for instance Tregoning *et al.* (2009).

Our approach is based on the three-cornered hat (TCH) method, which was proved efficient at estimating the precision of space geodesy techniques (Koot *et al.* 2006; Feissel-Vernier *et al.* 2007), and allows us to estimate the average precision of each technique, and to assess the impact of the modelling strategy on the precision by comparing several solutions for GRACE and GPS and different GCM combinations. We focus on Southern Europe, where (1) a dense network of GPS stations is available, (2) the Glacial Isostatic Adjustment (GIA) is negligible and (3) no strong non-tidal effects are expected (Boy & Lyard 2008).

The paper is organized as follows. We first describe the data sets and their processing in Section 1, and present the TCH method in Section 2. We then apply the method to the data and present the results in Section 3. Finally, in Section 4, we discuss our results, just before the conclusion in Section 6.

2 DATA USED AND PROCESSING

Farrell (1972) shows how to convert a global load distribution into ground displacement and gravity. As GRACE and GCMs models, unlike the GPS network used, are global, we convert them both into surface displacement using Farrell method, and using a spherical harmonic decomposition.

2.1 GPS

We use two GPS solutions over Europe. The first one, called here European combined, is a combination of a weekly reprocessing of the regional EUREF Permanent Network (EPN; Bruyninx 2004) performed at the Royal Observatory of Belgium, with weekly global International GNSS Service solutions (IGb, Paul Rebischung, personal communication, June 2011). The characteristics of these two solutions are summarized in Table 1. This combination is necessary as Legrand *et al.* (2012) demonstrated that the size of the network in regional GPS solutions induces an underestimation of the seasonal component up to about 30 per cent. As recommended by Collilieux *et al.* (2011), in order to mitigate network effects for this combination, no scale factor was estimated, and a stable well-distributed subnetwork, namely the IGS core network, was used during a two-step combination. The European reprocessing uses the Niell mapping function (Niell 1996), which has been proved to create spurious annual signals (Tregoning & Watson 2009). On the other hand, Fund *et al.* (2011) and Boehm *et al.* (2007) found that bias larger than 4 mm in Europe between solutions using Niell mapping function and up-to-date Vienna Mapping Function (VMF; Boehm *et al.* 2006), are concentrated at high latitudes. Consequently, the impact on this study should be limited. The second GPS solution is the ULR4 one (Santamaria-Gomez *et al.* 2011) from the Université de la Rochelle. It is a global, homogeneously reprocessed solution that uses up-to-date processing parameters, with a better-suited tropospheric delays mapping function, but has

a sparser spatial distribution. Technical information for the two solutions are provided in Table 1. Note that we only keep the stations with less than 25 per cent of gaps over the study time period (2002 August to 2009 May), for a total of 110 stations for the European combined solution and 36 for the ULR4 solution.

2.2 Space gravimetry

We use four GRACE geoid models solutions, produced by the Groupement de Recherches en Géodésie Spatiale (GRGS), GeoforschungsZentrum (GFZ), Center of Spatial Research (CSR) and Jet Propulsion Laboratory (JPL) teams. Their main characteristics, the pre-processing applied, and relevant references are described in Table 2. Except for the GRGS, the GRACE solutions are affected by striping noise (Chen *et al.* 2005), which needs to be filtered out. This filtering process was accomplished by applying to the original spherical harmonic geoid fields a Gaussian filtering of 500 km radius (Jekeli 1981; King *et al.* 2006), in addition to the decorrelation filter detailed by Swenson & Wahr (2006) with parameters from Duan *et al.* (2009). The atmosphere and ocean dealiasing (AOD) products, representing the non-tidal contributions of ocean and atmosphere, are added back into the GRACE spherical harmonic fields in order to be consistent with the GPS and GCM data. To ensure the consistency between the different geoid solutions, we also replaced the C_{20} coefficients from the CSR, JPL and GFZ models by a value obtained from SLR data, as suggested by Cheng & Tapley (2004). In the GRGS solution, the C_{20} coefficient is constrained from SLR measurements, and has consequently not been changed.

We then convert the geoid models into surface displacements at the GPS station positions, using the method described by Farrell (1972), using elastic load Love numbers in the Earth's centre of figure, computed for the PREM earth model (Pagiatakis 1990).

2.3 Loading models

The total load is estimated by the sum of the hydrology, ocean, and atmosphere contributions. We used two hydrological models (GLDAS and WGHM), two baroclinic ocean models (ECCO and Mercator) and the ground displacements computed from the NCEP reanalysis atmospheric model by Petrov & Boy (2004). Their characteristics and relevant references are summarized in Table 3. For GLDAS, the total water load is the sum of the soil moisture of the four layers and of the snow cover. Oceanic load in kg m^{-2} is directly estimated from Ocean Bottom Pressure data by dividing by a mean value of the gravity in m s^{-2} . Periods shorter than 1 month have been smoothed out by applying a running window average filter.

2.4 Reference frame

If the displacement estimates from GRACE, from GPS and from GCMs are not referred to the same origin, it generates errors, which can reach the same level as the precision we want to achieve. The GPS solutions are centred on the centre of the stations network, assumed to be the Earth's centre of figure. As described for example by Davis *et al.* (2004), the GRACE models have their origin at the Earth's centre of mass, and they have to be translated to the Earth's centre of figure. Here, we use for this translation the degree 1 coefficient of the load from the Swenson *et al.* (2008) geocentre model, following the procedure described, for example, by Nahmani *et al.* (2012) or Tregoning *et al.* (2009). We applied this same procedure to ensure the GCMs combinations to be referred to the Earth's centre of Figure.

Table 1. Main characteristics of the GPS solutions. Our European combined solution is a combination of the European and IGB solutions.

GPS solution	ULR4	European solution	IGb
Computation centre	Université de la Rochelle	Royal Observatory of Belgium	Institut National de l'Information Géographique et Forestière
Strategy	Ionosphere-free double differences, using dynamic subnetworks	Ionosphere-free double differences	Weekly combination of ionosphere-free solutions from 11 analysis centres
Software	Gamit 10.34	Bernese 5.0	The combination uses CATREF. The analysis centres use Bernese, Gamit, Gipsy-OASIS, EPOS, GINS or NAPEOS
Global or regional	Global	Regional	Global
Mapping function	VMF1	Niell	Most analysis centres use VMF1 or GMF
A priori zenithal hydrostatic delays	ECMWF	Standard Pression and Temperature	Most analysis centres use GPT
Tropospheric gradients	Two East/West and North/south gradients estimated per day	Two East/West and North/south gradients estimated per day	Most analysis centres estimate one pair of gradients per day and per station
Orbits	Re-estimated	IGS, not estimated	Re-estimated by analysis centres
Earth Orientation Parameters	Re-estimated	IGS, not estimated	Re-estimated by analysis centres
Solid earth tides	IERS 2003 conventions	IERS 2003 conventions	IERS 2003 conventions
Oceanic tides	FES2004	FES2004	FES2004
Atmospheric tides	Not used	Not used	Not used
Time span	1 week	1 week	1 week
Number of stations available with 75 per cent or more data	36	110	67
Reference	Santamaria-Gomez <i>et al.</i> (2011)	Bruyninx (2004)	Rebischung (personal communication)

Table 2. Main characteristics of the GRACE geoid models.

Research team	CNES/GRGS	CSR	GFZ	JPL
Release	RL02	RL04	RL04	RL04
Maximum degree	50	60	120	120
Ocean dealiasing model	MOG2D	OMCT	OMCT	OMCT
Atmosphere dealiasing model	ECMWF	ECMWF	ECMWF	ECMWF
Reference	Bruinsma <i>et al.</i> (2010)	Bettadpur (2007)	Flechtner <i>et al.</i> (2010)	Watkins & Yuan (2007)
Filtering	None	Gaussian filtering, radius 500 km + decorrelation filter from Swenson <i>et al.</i> (2006) with parameters from Duan <i>et al.</i> (2009)		

Table 3. Main characteristics of the GCMs used.

Contribution	Hydrology		Ocean		Atmosphere
	GLDAS	WGHM	ECCO	Mercator	NCEP
Data modelled	Surface and subsurface soil moisture (kg/m ²)	Surface, subsurface soil moisture and large surface aquifers water load (kg/m ²)	Ocean bottom Pressure under IB hypothesis (Pa)	Ocean bottom Pressure under IB hypothesis (Pa)	Pressure loading associated displacement (mm). IB hypothesis over the oceans, including the Mediterranean sea.
Time span	1 month	1 month	10 days	1 week	6 hours
Grid step	0.25°	0.5°	Interpolated at 1°, using spline interpolation	Interpolated at 1°, using spline interpolation	2.5°
Reference	Rodell <i>et al.</i> (2004)	Döll <i>et al.</i> (2003)	Lee <i>et al.</i> (2002)	Drillet (personal communication)	Petrov & Boy (2004)

2.5 Total and interannual displacements

The periods shorter than 1 month were filtered out using a running average, and the time-series were sampled to a common monthly time span. In addition, we estimated and removed the trend from all the time-series as, for GPS, it includes tectonic contributions.

The geophysical signal remaining in the pre-processed data sets is dominated by the seasonal cycle (Fig. 1). This is not optimal for our purpose as it can include sources other than the water load, especially for the GPS. For example, the seasonal temperature fluctuations can create an annual signal in the antenna position due to thermal expansion of the bedrock or of the building, or to phase centre variations (Dong *et al.* 2002). Consequently, we also investigate separately the interannual cycle. This interannual signal is obtained by subtracting from each time-series a composite annual cycle and by applying a low-pass filter to all these residual time-series (Fig. 2), removing periods smaller than 6 months. The composite annual

cycle is computed as the mean seasonal signal over the entire time span: the January value of the composite is the mean value in January over all the time-series (Hartmann & Michelsen 1989).

3 THE TCH METHOD

3.1 Basic principle of the TCH method

The TCH method aims to estimate the precision of three measurement techniques observing the same quantity, under the hypothesis that the errors of each technique are independent from the errors of the others (Premoli & Tavella 1993). For a given observation time-series, D_i , one can write:

$$D_i = D_{\text{true}} + \varepsilon_i, \quad (1)$$

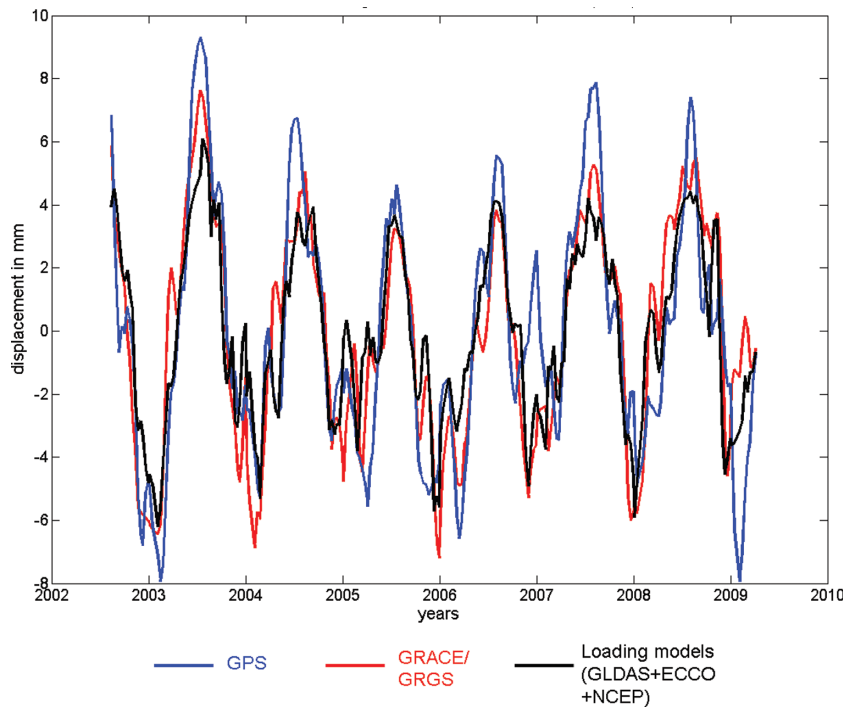


Figure 1. Time-series of vertical displacement at the Matera station (mm) from GRACE-GRGS (red), GPS (European combined solution, blue) and the sum of the loading models (GLDAS+ECCO+NCEP, black).

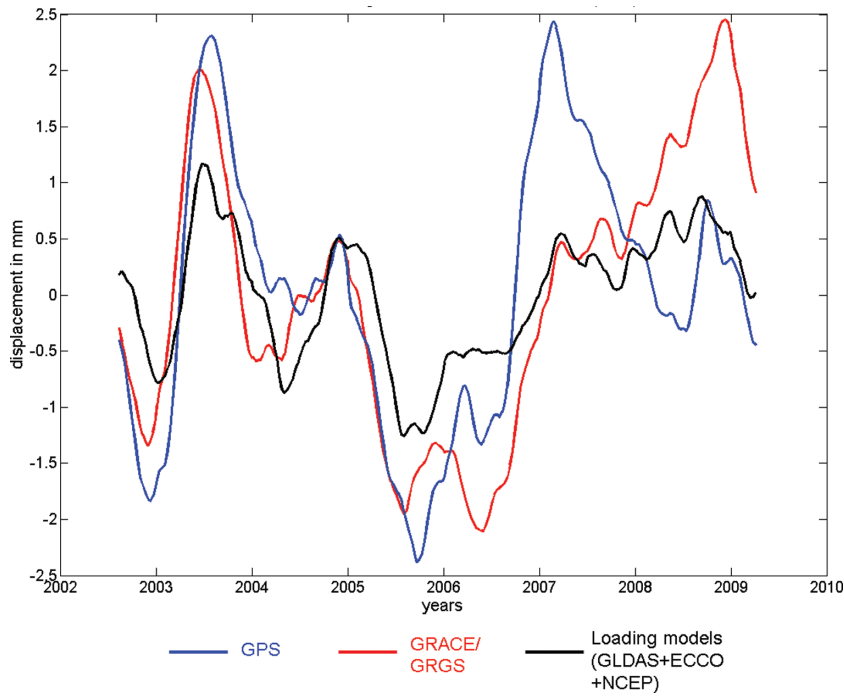


Figure 2. Time-series of interannual vertical displacement at the Matera station (mm) from GRACE-GRGS (red), GPS (European combined solution, blue) and the sum of the loading models (GLDAS+ECCO+NCEP, black).

where D_i is the time-series of displacement as determined from the data of the technique i , D_{true} is the true displacement, which is common to all the techniques and ε_i the error of technique i . For each station, each solution is then the exact sum of the displacement due to the water load, common to all the solutions and techniques, and of the residual term, which only depends on the technique, solution and station. In our case, the three techniques do not exactly observe the same signal, and a part of the ‘error’ is actually a signal that the others do not see, such as the local deformation that only GPS can measure. For the sake of clarity, in what follows, we will nevertheless speak about error. Computing the variance of the difference between the time-series from two techniques i and j , we obtain:

$$\begin{aligned} \text{var}(D_i - D_j) &= \text{var}(D_{\text{common}} + \varepsilon_i - D_{\text{common}} - \varepsilon_j) \\ &= \text{var}(\varepsilon_i - \varepsilon_j) \\ &= \text{var}(\varepsilon_i) + \text{var}(\varepsilon_j) - 2\text{cov}(\varepsilon_i, \varepsilon_j). \end{aligned} \quad (2)$$

For techniques i and j with independent errors, the covariance between their errors is zero and

$$\text{var}(D_i - D_j) = \text{var}(\varepsilon_i) + \text{var}(\varepsilon_j). \quad (3)$$

When three data sets with independent errors are used, the eq. (3) make a set of three equations with three unknowns, with a unique solution: the three variances of the technique errors. This is actually the case when using three independent sources of information: GPS, GRACE and the sum of the GCMs.

Note that this hypothesis of null covariance is only true at the first order as, for instance, the same atmospheric and oceanic products are used in the dealiasing of GRACE and in GPS analysis. This point is discussed in Section 3.2, where we justify this approximation.

3.2 Example of the Matera station, Italy

Fig. 1 shows the time-series of vertical displacement computed from GRACE-GRGS, GPS and the sum of loading models GLDAS + ECCO + NCEP for the Matera station (MATE), Italy.

For this station, we applied the TCH equation system (eq. 3) to the vertical displacements from one GRACE solution (GRACE-GRGS time-series), one GPS solution (European combined time-series) and one combination of loading models (the time-series of the sum of GLDAS, ECCO and NCEP contributions). We obtain the standard deviation of the error as 0.8, 1.7 and 0.6 mm for, respectively, the GRACE, the GPS and the load models solutions (Table 5). These results are smaller than the amplitude of the computed displacements (Fig. 2), confirming that a large part of the signal is common to the GRACE, GPS and the sum of the models.

Over the interannual part of the signal, the error standard deviation is found to be 0.4, 0.8 and 0.5 mm for the considered GRACE, GPS and the load models solutions, respectively (Table 6). Note that this error reduction mostly results from the running average, as averaging on 6 values diminishes the standard deviation by a factor of $2.4(\sqrt{6})$.

4 RESULTS

We have three independent sources of information, GPS, GRACE and load models, with several solutions for each technique. Section 2.2 has presented a basic application of the TCH on one station, with only one solution for each technique. In this Section 3, we use the full data set, that is, the four GRACE solutions, the four combinations of the GCMs and the two GPS solutions, for all the stations of our network. By computing the variances of the differences between two time-series of displacement on each station, we can write the equation system for all pairs of series. We keep and estimate the covariance term when we consider the differences of time-series between two solutions of the same technique, like two

GRACE solutions, and we set this covariance term to zero in case of two different techniques, as mentioned in Section 2.1 (eq. 3). The resulting system remains over-determined and is solved by a least-square procedure. This approach is consistent with the method of Chin *et al.* (2005), who showed that the TCH method has a solution even when data sets with correlated error are used, as long as there are at least three differences of time-series from techniques with independent errors, which is the case here as we have several solutions from each one of our independent techniques. The covariance that need to be estimated are those between two solutions of the same technique. As some techniques have more observations than others, we weight the equations so that, globally, every technique (GRACE, GPS and models) is given the same weight in the total system.

Considering that the time-series from each data set at each station allow sampling the error of the technique used to generate the time-series, we solve, in part A, a global equation system with only three unknown variances: the error variance of GRACE, GPS and the sum of the loading models. Then, considering that the time-series from each solution at each station allow us to sample the error of a given solution, we compare, in part B, the solutions from the same technique with each other. In this case, the number of unknown variances equals 10 (four GRACE solutions, four combinations of the loading models and two GPS solutions). Finally, in part C, we solve the same equation system, with the same unknowns than in part B, but for each station independently. This allows to detect geographical patterns in the precision of a given solution, as well as local anomalies.

4.1 Technique level comparison

To obtain the technique error, we only use differences of time-series from different techniques. We do not consider the differences between two solutions of a same technique, as they are supposed here to be the samplings of the same quantity, the technique error. The system is then composed of 32 equations for each station, or 24 if the station is not part of the ULR4 solution (see Table 4). The 32 equations are the 16 differences between the time-series of each one of the two GPS solutions and each one of the four GRACE solutions and of the four combinations of models, in addition to the 16 differences between each one of the four GRACE solutions and each one of the four GCM solutions. We solve the global system for the variance of the errors for GRACE, GPS and the loading models. In order to get better estimations of the uncertainties on the error variances, we used a boot-strapping method with 1000 resamplings (Moore *et al.* 2003), randomly picking as many stations as in the initial set, with repetition, and making independent estimation of the errors for each resampling. The medians, extreme values, and standard deviations for the errors are presented in Fig. 4. The results are at the same order than those obtained for the Matera station, with error standard deviation for the vertical displacement of 1.2, 2.1 and 1.0 mm for GRACE, GPS and the loading models, respectively. Note that 1 mm of vertical displacement corresponds to about 2 cm of equivalent water height at a 2500 km spatial scale (Fig. 3). Similar conclusions hold for the interannual vertical errors, though the standard deviations are half the size: 0.5 mm for the loading models, 0.6 mm for GRACE and 1.1 mm for GPS. The relative errors, representing the ratios between the variances of the errors and the variances of the signals, are shown on Fig. 5. Both on total and interannual signals, for GRACE, GPS and the loading models, these relative errors are always smaller than 50 per cent, showing

that a significative part of the variance of the signal can be explained by the common loading, included at interannual timescale.

4.2 Solution level comparison

We also use the TCH method to compare the quality of the different solutions for a same technique, by estimating the variance of the error term for each solution. In this case, the equations with differences of time-series from the same techniques are added into the system described in Section 3.1. The covariance between the errors for two solutions of a same technique are kept as an unknown of the system and estimated. This leads to 13 equations more than in Section 3.1 or 12 if the station is not part of ULR4 solution. These 13 equations are the six pair-wise differences between the four GRACE solutions, the six pair-wise differences between the four combinations of GCMs and the difference between the two GPS solutions time-series if the station is part of the ULR4 solution. We then have 36 equations on each station, and 45 for stations included in the ULR4 Solution (Table 4). Tables 7 and 8 present the results obtained, respectively, on the total and interannual time-series. Both on the total signal and on the interannual displacements, our results show that the standard deviation of the errors depends more on the technique than on the solution used.

As mentioned above, there might be some covariance between the intertechnique errors. Including all the covariance as unknown of the problem would make it underdetermined. To overcome that problem, we added constraint equations, under the hypothesis of weak correlation for all the intertechniques errors. The obtained results with this method are consistent within 0.2 mm with the results presented in Tables 7 and 8, confirming that the possible intertechnique covariance can be left out of the problem.

4.2.1 Comparison of the GPS solutions

In Table 7, the precision of the ULR4 solution appear slightly better than that of the European combined one. Nevertheless, if we restrict the estimation on the ULR4 stations only, the results for the two solutions are both at 1.9 mm. This indicates that the difference resulted mostly from the different network, as the ULR4 network is less homogeneously distributed than the network of 110 stations of the European combined solution. This also implies that the impact of the differences in data processing strategy is small with respect to the intertechnique differences.

4.2.2 Comparison of the GRACE solutions

The estimated precision for the GRACE solutions is at the same order, about 1 mm. The best precision is obtained with the GRGS model. This is appears to be due to the fact that the amplitudes of the displacements from the GRGS solution are generally slightly larger than for the other solutions, and more consistent with those from the GCMs and the GPS. Also note that the GRGS solution is less covariant with the other GRACE solutions than the other GRACE models with each other. This point is consistent with the differences in data processing methods, and in particular the stabilization applied to the GRGS solution in order to avoid any additional data filtering (Bruinsma *et al.* 2010). This difference disappears at interannual timescale, the four GRACE solutions giving similar errors.

Table 4. Summary of the number of equations and of the number of unknowns in the three-cornered hat system. Each line corresponds to a way of solving the three-cornered hat system, the second column corresponds to the total number of observations (i.e. equations) of the three-cornered hat system, the third column is the number of total estimated parameters (i.e. the variance of the residuals and the covariance of the residuals between two solutions for a same technique), and fourth and fifth columns are respectively the total number of variances and covariance (including usually non-estimated intertechnique covariance).

Level of resolution (and concerned section)	Estimated variance of residuals	Number of equations	Number of variances	Total number of covariance	Total number of unknowns	Number of covariance considered as null
Basic case (1 GPS solution, 1 GRACE solution, 1 model solution), at the station level (Section 2.2)	One variance of residual for each data	3 (for one station)	3	3 (all are intertechnique covariance)	3 (3 variances)	3 (all differences are intertechnique differences, no differences between two solutions of the same technique)
At the technique level (Section 3.1)	One variance of residual for each technique (case 1)	24 × 36 stations (where we have 2 GPS solutions) + 36 × 74 stations (where we have only one GPS solution) = 3528 (only intertechnique differences are considered at this level)	3	3 (all are intertechnique covariance)	3 (3 variances)	3 (all differences are intertechnique differences, no differences between two solutions of the same technique)
At the solution level (Section 3.2), case 1 (stations part of European combined GPS solution only)	One variance of residuals for each solution,	36 × 74 stations + = 4284	10	45	23 (10 variances + 13 covariance between different solutions of the same technique)	32 (the intertechnique covariance)
At the solution level (Section 3.2), case 2 (stations being part of European combined and ULR4 GPS solutions)	One variance of residuals for each solution	45 × 36 stations				
At the station level (Section 3.3)	One variance of residuals for each solution and for each station (case 3)	36 (for each of the 74 stations only part of European combined solution)	9 (for one station)	36 (for one station)	21 (for one station): 9 variances + 12 covariance	24 intertechnique covariance (for one station)
		45 (for each of the 36 stations part of European combined and of ULR4 solutions)	10 (for one station)	45 (for one station)	23 (for one station): 10 variances + 13 covariance	32 intertechnique covariance (for one station)
Generalized three-cornered hat, at the station level	One variance of residuals and all covariance for each solution and each station	36 + 24 constraint equations (for each one of the 74 stations only part of European combined solution) = 60	9 (for one station)	36 (for one station)	45 (for one station)	None (all covariance, even intertechnique ones, are estimated)
		45 + 32 constraint equations (for each of the 36 stations part of European combined and of ULR4 solutions) = 77	10 (for one station)	45 (for one station)	55 (for one station)	

Table 5. Standard deviation of the errors on the vertical displacements at the Matera station.

	GRACE GRGS	GPS European combined	Loading models GLDAS+ ECCO+ NCEP
Standard deviation of residuals (mm)	0.8	1.7	0.6

Table 6. Standard deviation of the errors on the interannual vertical displacements at the Matera station.

	GRACE GRGS	GPS European combined	Loading models GLDAS+ ECCO+ NCEP
Standard deviation of residuals (mm)	0.4	0.8	0.5

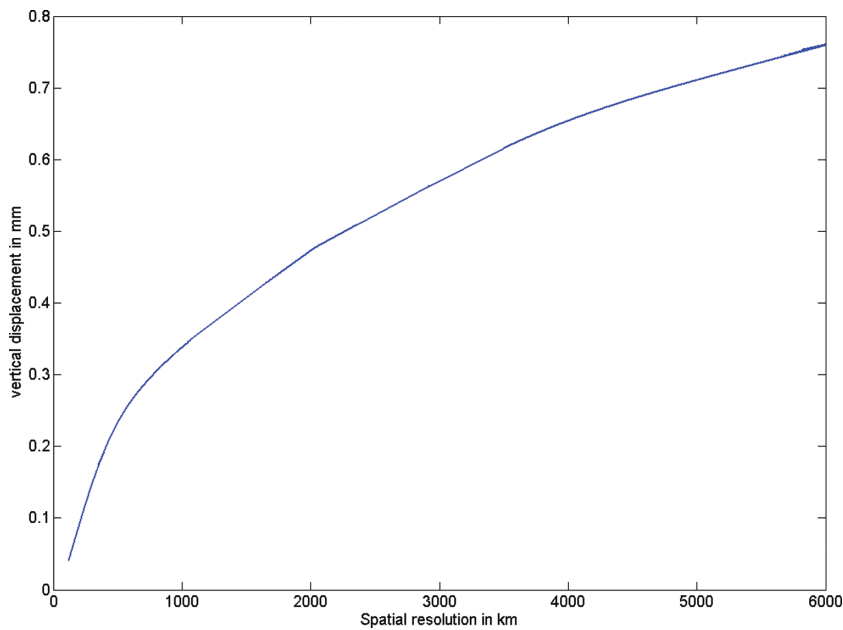


Figure 3. Vertical displacement induced by a 1 cm equivalent water height loss, as a function of the spatial scale of this load.

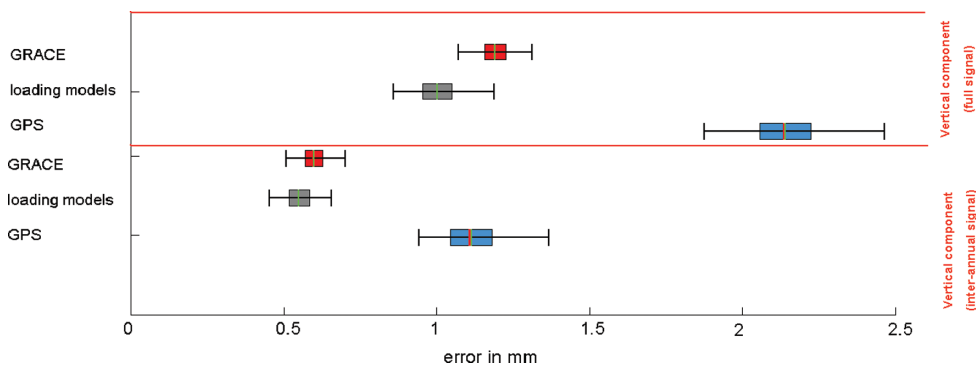


Figure 4. Standard deviation of the residuals computed by the three-cornered hat method. Results are given at the technique level (GRACE, GPS, loading models), for the Vertical, Eastern, Northern and interannual Vertical displacements. The half length of the thick coloured bars represents the standard deviation of the residual estimates obtained from the bootstrapping method, the green vertical bar the median value (assumed to be the standard deviation of the residual) and the two extremes of each thin bar the minimal and maximal value obtained when doing the bootstrapping.

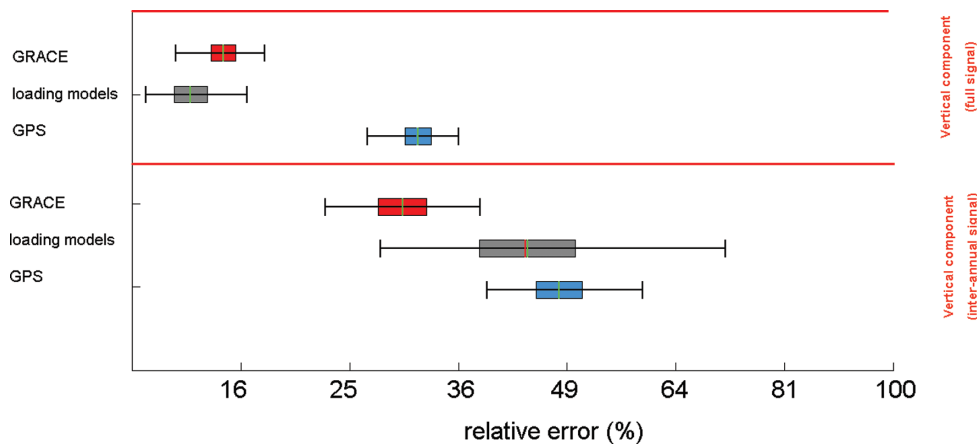


Figure 5. Relative residuals (ratio between the variance of the residuals computed by the three-cornered hat method and the mean variance of the signal). Results are given at the technique level (GRACE, GPS, loading models), for the Vertical, Eastern, Northern and interannual Vertical signals.

Table 7. Standard deviation of the errors in mm (diagonal terms) and correlation of the errors (non-diagonal terms) on the vertical displacements on the 110 European stations. Grey blocks indicate that the intertechnique covariance of the residual terms are not estimated.

	GRACE-GRGS	GRACE-JPL	GRACE-CSR	GRACE-GFZ	GPS (European combined)	GPS (ULR4) on 36 stations only	GLDAS+ ECCO+ NCEP	GLDAS+ Mercator+ NCEP	WGHM+ ECCO+ NCEP	WGHM+ Mercator+ NCEP
GRACE-GRGS	1.0 ± 0.06	0.10	0.29	0.39						
GRACE-JPL		1.4 ± 0.06	0.86	0.83						
GRACE-CSR			1.2 ± 0.06	0.82						
GRACE-GFZ				1.3 ± 0.06						
GPS (European combined)					2.1 ± 0.13	0.71				
GPS (ULR4) on 36 stations only						1.9 ± 0.09				
GLDAS+ ECCO+ NCEP							0.8 ± 0.05	0.61	0.60	0.49
GLDAS+ Mercator+ NCEP								0.9 ± 0.05	0.52	0.88
WGHM+ ECCO+ NCEP									1.0 +/- 0.06	0.95
WGHM+ Mercator+ NCEP										1.1 +/- 0.06

Table 8. Standard deviation of the errors in mm (diagonal terms) and correlation of the errors (non-diagonal terms) on the interannual vertical displacements on the 110 European stations. Grey blocks indicate that the intertechnique covariance of the residual terms are not estimated.

	GRACE-GRGS	GRACE-JPL	GRACE-CSR	GRACE-GFZ	GPS (European combined)	GPS (ULR4) on 36 stations only	GLDAS+ ECCO+ NCEP	GLDAS+ Mercator+ NCEP	WGHM+ ECCO+ NCEP	WGHM+ Mercator+ NCEP
GRACE-GRGS	0.6 ± 0.04	0.56	0.65	0.73						
GRACE-JPL		0.6 ± 0.04	0.89	0.71						
GRACE-CSR			0.6 ± 0.04	0.69						
GRACE-GFZ				0.6 ± 0.04						
GPS (European combined)					1.2 ± 0.10	0.69				
GPS (ULR4) on 36 stations only						1.1 ± 0.07				
GLDAS+ ECCO+ NCEP							0.5 ± 0.04	0.87	0.79	0.64
GLDAS+ Mercator+ NCEP								0.6 ± 0.05	0.68	0.98
WGHM+ ECCO+ NCEP									0.6 ± 0.05	0.97
WGHM+ Mercator+ NCEP										0.7 ± 0.05

4.2.3 Comparison of the loading models combinations

The precisions of the GCM combinations are also of the same order, about 1.2 mm, with small differences between the combinations: for example WGHM and Mercator generate about 0.4 mm more standard deviation of errors than GLDAS and ECCO, which give the best results. This suggests that the use of that combination might be optimal for comparing with geodesy data.

4.3 Station level comparison of the solutions

When solving the same equation system for each station independently, we obtain information on the precision of each solution at each station as shown on Fig. 6, and on Fig. 7 for the interannual signal.

The GRGS and CSR solutions, which appear to be the most precise ones in the previous section, do not show any clear geographical

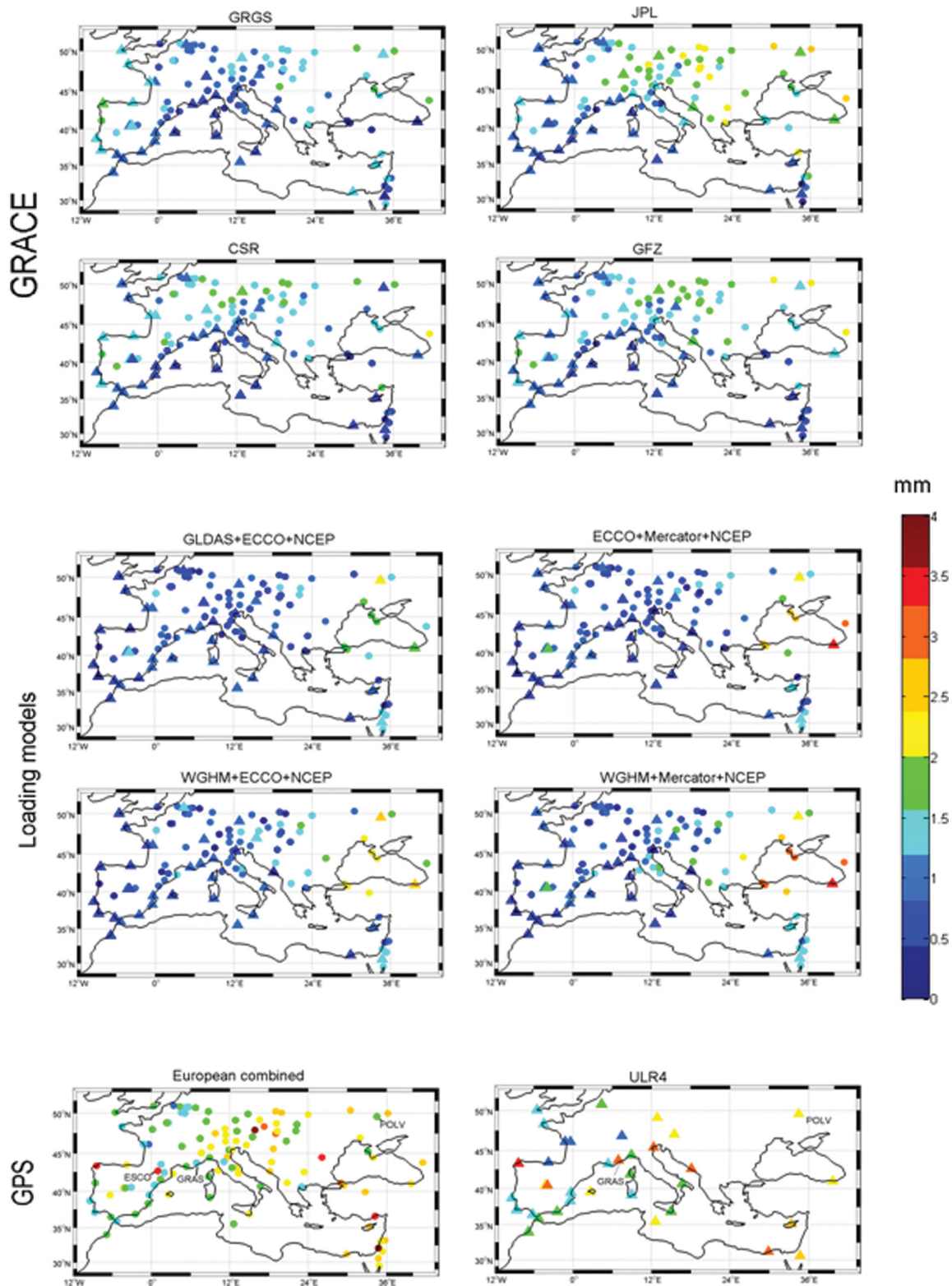


Figure 6. Maps of residuals on the vertical displacements due to the loading (in mm) given by station and by solution.

pattern in their local errors. Conversely, a consistent spatial pattern appears in the errors estimated for the GFZ or JPL models, with higher errors in Eastern Europe (Ukraine, Romania) and in the Atlantic coast than in the Mediterranean region. In coastal regions, this result can be due to the non-homogeneous quality of the dealiasing product, whereas in Eastern Europe it might be mainly due to a

slightly smaller amplitude of the annual signal in those GRACE solutions.

Spatial patterns also appear in the map of errors on the load mass estimation derived from the loading models: larger errors are found around the Black Sea. This would indicate a less precise modelling of the Black Sea Ocean Bottom Pressure. The distribution

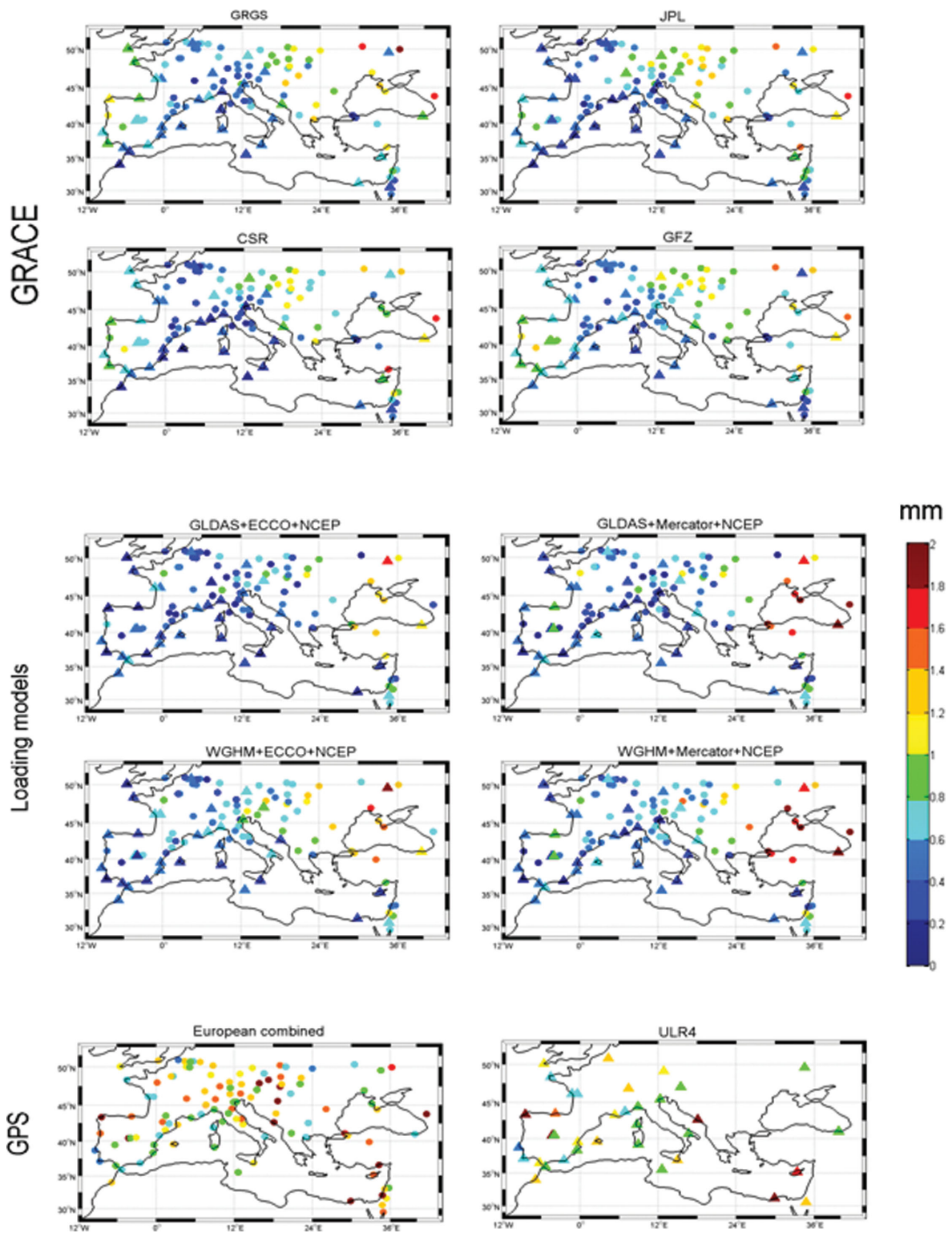


Figure 7. Maps of residuals on the interannual vertical displacements due to the loading (in mm) given by station and by solution.

of estimated GPS standard deviations of errors shows higher values in the Middle-East and in some Eastern Europe stations. Stations with strong local effects appear clearly, such as ESCO station in the Spanish Pyrenees where effects due to the high altitude (around 2450 m) can affect the amplitude of annual signal. This suggests a practical application of this method for the detection of anomalies in the GPS time-series.

5 DISCUSSION

Using the TCH method on GPS, GRACE and climate GCMs, we estimate the load deformation precision at the mm level for GRACE and the GCM, and twice as large for the GPS. Note that this precision estimates does not only include the specific technique and solution errors in measuring the deformations, the gravity changes,

or in estimating the mass associated to water load, that is, what we actually want to estimate, as they also include the possible geophysical contributions other than the common water signal, as well as the omission error related to the difference of spatial resolution of the water load estimation between the different techniques.

The other geophysical contributions are actually not an issue for our study, as we want to investigate the quality of the water load determination; consequently, considering such contributions as error is appropriate. In addition, those effects are expected to be small. Indeed, we removed a trend for all the data sets, the time-series should be free from any linear tectonic, GIA or subsidence (Zerbini *et al.* 2007) signals. Moreover, earthquakes effects should not be present in our time-series as de Viron *et al.* (2008) showed that GRACE was only able to detect earthquakes with a magnitude larger than 8.6, which did not happen in our area of interest, and as earthquakes-related discontinuities have been removed from the GPS time-series during the stacking step. Given the earthquakes which occurred between 2002 and 2009, residual post-seismic displacements can locally affect significantly GPS time-series on some stations in the area of the epicentres, especially in Central and Southern Italy (earthquake of l'Aquila in 2009) and Morocco (earthquake of Al-Hoceima in 2004). The number of stations concerned is however limited. The GPS time-series also include local site effects, for instance linked with seasonal deformations of the buildings where stations are installed, displacements due to monumentation instability (Dong *et al.* 2002), or local geologic effects (Nahmani *et al.* 2012).

As the displacements from both GRACE and the models have a space resolution of the order of several hundreds of kilometres, the omission error on the displacements associated to water load is mostly associated with the shorter wavelengths spatial signal in the GPS station positions, which is not present in GRACE and the models. Note that the conversion from loading to displacements also acts as a low-pass filter: the resulting displacement from a load is more sensitive to low frequencies than to local spatial patterns, compared to the original load. Therefore the differences of resolutions between the three techniques are smaller when considering the displacements than one could expect from the difference of a priori resolutions.

For the GPS, specific technique and solution errors may come from the propagation of mismodellings in zenithal hydrostatic a priori delays, mapping function, antenna phase centre variations, solid or oceanic tides or orbits, draconitic signals (Ray *et al.* 2008), multipaths effects, or the fact that atmospheric tides are not taken into account (van Dam *et al.* 2007; Tregoning & Watson 2009). For GRACE, those are mostly related to aliasing noise. For the loading models, they would be associated with the modelling errors or the non-modelled contributions, like groundwater in hydrological models or great surface aquifers, which are not taken into account in GLDAS.

When considering that the load mass from GRACE has a mean spatial scale of 2500 km, the 1.2 mm precision obtained here corresponds to about 2.5 cm of water height, which is consistent with previous studies. Estimates obtained by Wahr *et al.* (2006) range between 2 and 3.5 cm of EWH. Swenson *et al.* (2006) found a precision of the GRACE-estimated water storage at the level of 2.5 cm EWH over large hydrological basins. A precision of 2 cm EWH was found by Klees *et al.* (2008) by comparing several global and regional GRACE solutions on basins larger than 1 million km², and by Longuevergne *et al.* (2010) over small basins.

Our error levels for the GPS displacements are smaller than the precision estimates obtained by Collilieux *et al.* (2010), who

reported a 4.7 mm precision based on a weekly repeatability analysis. Our results are consistent with those of Ray (2011), who found a 2.2 mm weekly repeatability on the vertical displacement at stations where the water signal is supposed to have been removed. The lesser precision of the GPS as compared to GRACE and the GCMs can be associated with local deformations, which are only measured by GPS, and by error from the technique itself. As shown by van Dam *et al.* (2007), the contribution of local load, or omission error, to this difference of errors between GPS and the two other techniques is expected to be small. However, our results also show that the GPS keeps a fair sensitivity to the water load also at interannual timescales.

The inconsistencies between geodetic measurements and the loading models in coastal areas, especially in the Atlantic, had been noticed by several studies (e.g. van Dam *et al.* 2007; Tesmer *et al.* 2011). A possible explanation is the large amplitude of oceanic tides at those locations, associated with the low amplitude of the annual signal. The use of imperfect tide correction models, assimilated in different ways in the GPS and GRACE data processing, may create artefacts contaminating the times-series.

6 CONCLUSION

We showed that the TCH can be used to assess the precision of the water load determined from GRACE, GPS and GCMs. We found that GRACE and the GCMs, when converted into vertical displacement, reach a precision of about 1mm over Europe, whereas the GPS performs with about twice this level of error. We also investigated the interannual signal, and showed that the performances of the different techniques are comparable to what is obtained for the seasonal signal. In particular, the GPS time-series keep a fair sensitivity to water load signals at interannual timescales, and the loading models prove to be efficient at retrieving the interannual water displacements. An outcome of our analysis was also to detect local problems in the different solutions, such as outlying GPS stations, or mismodelling of the Black Sea. When comparing different solutions for each type of data/model, we assessed the impact of the processing strategy of each GRACE and GPS time-series and compared the quality of the different loading models. Both on the total and on the interannual displacements, it was shown that the standard deviation of the errors depended more on the technique than on the solution used. In the future, this assessment can be completed by studies at a global scale, as a step towards a possible use and assimilation of geodetic data into hydrological and oceanic circulation models.

ACKNOWLEDGEMENTS

We are grateful to Xavier Collilieux and to the two reviewers for their remarks and fruitful discussions. The help of Arthur Jacobs and Wayne Crawford in the editing of the paper is gratefully acknowledged. We thank CNES for financial support through the TOSCA program, as an exploitation of the GRACE mission. This study was supported by the Institut Universitaire de France. We thank the GLDAS, ECCO, NCEP and WGHM teams for the GCMs outputs used in this work. We also thank Yann Drillet and the Mercator team for providing us the Mercator ocean model, and the editor and reviewers for their remarks and comments, which helped us to improve this manuscript.

REFERENCES

- Bettadpur, S., 2007. CSR Level-2 processing standards document for level-2 product release 0004, GRACE 327742 (Rev. 3.1).
- Blewitt, G., Lavalée, D., Clarke, P. & Nurutdinov, D., 2001. A new global mode of Earth deformation: seasonal cycle detected, *Science*, **294**, 2342–2345.
- Blewitt, G. & Clarke, P., 2003. Inversion of Earth's changing shape to weigh sea level in static equilibrium with surface mass redistribution, *J. geophys. Res.*, **108**(B6), 2311, doi:10.1029/2002JB002290.
- Boehm, J., Werl, B. & Schuh, H., 2006. Troposphere mapping functions for GPS and very long baseline interferometry from European Centre for Medium-Range Weather Forecasts operational analysis data, *J. geophys. Res.*, **111**, B02406, doi:10.1029/2005JB003629.
- Boehm, J., Mendes Cerveira, P.J., Schuh, H. & Tregoning, P., 2007. The impact of tropospheric mapping functions based on numerical weather models on the determination of geodetic parameters, in *Dynamic Planet—Monitoring and Understanding a Dynamic Planet with Geodetic and Oceanographic Tools*, Vol. 130, pp. 837–843, eds Tregoning, P. & Rizos, C., Springer, International Association of Geodesy Symposia, doi:10.1007/978-3-540-49350-1_118.
- Boy, J.-P. & Lyard, F., 2008. High-frequency non-tidal ocean loading effects on surface gravity measurements, *Geophys. J. Int.*, **175**, 35–45.
- Bruinsma, S., Lemoine, J.-M. & Biancale, R., 2010. CNES/GRGS 10-day gravity field models (release 2) and their evaluation, *Adv. Space Res.*, **45**(4), 587–601.
- Bruyninx, C., 2004. The EUREF Permanent Network: a multi-disciplinary network serving surveyors as well as scientists, *Geoinformatics*, **7**, 32–35.
- Chambers, D.P., 2006. Evaluation of new GRACE time-variable gravity data over the ocean, *Geophys. Res. Lett.*, **33**, L17603, doi:10.1029/2006GL027296.
- Chen, J.L., Wilson, C.R., Famiglietti, J.S. & Rodell, M., 2005. Spatial sensitivity of GRACE time-variable gravity observations, *J. geophys. Res.*, **110**, B08408, doi:10.1029/2004JB003536.
- Cheng, M. & Tapley, B.D., 2004. Variations in the Earth's oblateness during the past 28 years, *J. geophys. Res.*, **109**, B09402, doi:10.1029/2004JB003028.
- Chin, T.M., Gross, R.S. & Dickey, J.O., 2005. Multi-reference evaluation of uncertainty in Earth orientation parameter measurements, *J. Geod.*, **79**(1–3), 24–32.
- Collilieux, X., Métivier, L., Altamimi, Z., van Dam, T. & Ray, J., 2010. Quality assessment of GPS reprocessed terrestrial reference frame, *GPS Solut.*, **15**(3), 219–231.
- Collilieux, X., van Dam, T., Ray, J., Coulot, D., Métivier, L. & Altamimi, Z., 2011. Strategies to mitigate aliasing of loading signals while estimating GPS frame parameters, *J. Geod.*, doi:10.1007/s00190-011-0487-6.
- Davis, J.L., Elosequi, P., Mitrovica, J.X. & Tamisiea, M.E., 2004. Climate driven deformation of the solid Earth from GRACE and GPS, *Geophys. Res. Lett.*, **31**(24), L24605, doi:10.1029/2004GL021435.
- Döll, P., Kaspar, F. & Lehner, B., 2003. A global hydrological model for deriving water availability indicators: model tuning and validation, *J. Hydrol.*, **270**, 105–134.
- Dong, D., Fang, P., Bock, Y., Cheng, M.K. & Miyazaki, S., 2002. Anatomy of apparent seasonal variations from GPS-derived site position time series, *J. geophys. Res.*, **107**(B4), doi:10.1029/2001JB000573.
- de Viron, O., Panet, I., Mikhailov, V., Van Camp, M. & Diament, M., 2008. Retrieving earthquake signature in GRACE gravity solutions, *Geophys. J. Int.*, **174**(1), 14–20.
- Duan, X.J., Guo, J.Y., Shum, C.K. & van der Wal, W., 2009. On the post-processing removal of correlated errors in GRACE temporal gravity field solutions, *J. Geod.*, **83**, 1095–1106.
- Famiglietti, J.S. et al., 2011. Satellites measure recent rates of groundwater depletion in California's Central Valley, *Geophys. Res. Lett.*, **38**, L03403, doi:10.1029/2010GL046442.
- Farrell, W.E., 1972. Deformation of the earth by surface loads, *Rev. geophys. Space Phys.*, **10**(3), 761–797.
- Feissel-Vernier, M., de Viron, O. & Le Bail, K., 2007. Stability of VLBI, SLR, DORIS, and GPS positioning, *Earth Planets Space*, **59**, 475–497.
- Flechtner, F., Dahle, C., Neumayer, K.-H., König, R. & Foerste, C., 2010. The release 04 CHAMP and GRACE eigen gravity field models, in *System Earth via Geodetic-Geophysical Space Techniques*, pp. 41–58, eds Flechtner, F., Gruber, T., Güntner, A., Mandea, M., Rothacher, M., Schöne, T. & Wickert, J., Springer-Verlag, Berlin, Heidelberg.
- Fund, F., Morel, L., Mocquet, A. & Boehm, J., 2011. Assessment of ECMWF-derived tropospheric delay models within the EUREF Permanent Network, *GPS Solut.*, **15**, 39–48.
- Güntner, A., Stuck, J., Werth, S., Döll, P., Verzano, K. & Merz, B., 2007. A global analysis of temporal and spatial variations in continental water storage, *Water Resour. Res.*, **43**, W05416, doi:10.1029/2006WR005247.
- Hartmann, D.L. & Michelsen, M.L., 1989. Intraseasonal periodicities in Indian rainfall, *J. Atmos. Sci.*, **46**(18), 2838–2862.
- Jekeli, C., 1981. *Alternative methods to smooth the Earth's gravity field*, Department of Geodetic Science and Surveying, Ohio State University, Columbus, Ohio, 48 pp.
- King, M., Moore, P., Clarke, P. & Lavallée, D., 2006. Choice of optimal averaging radii for temporal GRACE gravity solutions, a comparison with GPS and satellite altimetry, *Geophys. J. Int.*, **166**, 1–11.
- Klees, R. et al., 2008. A comparison of global and regional GRACE models for land hydrology, *Surv. Geophys.*, **29**, 335–359.
- Koot, L., de Viron, O. & Dehant, V., 2006. Atmospheric angular momentum time-series: characterization of their internal noise and creation of a combined series, *J. Geod.*, **79**(12), 663–674.
- Legrand, J., Bergeot, N., Bruyninx, C., Wöppelmann, G., Santamaria-Gomez, A., Bouin, M.-N. & Altamimi, Z., 2012. Comparison of regional and global GNSS positions, velocities and residual time series, in *Proceedings of the International Association of Geodesy Symposia* Vol. 136, *Geod. Planet Earth*, pp. 95–104.
- Lee, T., Fukumori, I., Menemenlis, D., Xing, Z.F. & Fu, L.L., 2002. Effects of the Indonesian throughflow on the Pacific and Indian Oceans, *J. Phys. Oceanogr.*, **32**, 1404–1429.
- Longuevergne, L., Scanlon, B.R. & Wilson, C.R., 2010. GRACE hydrological estimates for small basins: evaluating processing approaches on the High Plains Aquifer, USA, *Water Resour. Res.*, **46**, W11517, doi:10.1029/2009WR008564.
- Moore, D.S., McCabe, G.P., Duckworth, W.M. & Sclove, S.L., 2003. *The Practice of Business Statistics: Using Data for Decisions*, 2nd edn, WH Freeman, New York, 859 pp.
- Nahmani, S. et al., 2012. Hydrological deformation induced by the West African Monsoon: comparison of GPS, GRACE and loading models, *J. geophys. Res.*, **117**(B05409), doi:10.1029/2011JB009102.
- Niell, A.E., 1996. Global mapping functions for the atmosphere delay at radio wavelengths, *J. geophys. Res.*, **101**(B2), 3227–3246.
- Pagiatakis, S.D., 1990. The response of a realistic Earth to ocean tide loading, *Geophys. J. Int.*, **103**, 541–560.
- Petrov, L. & Boy, J.-P., 2004. Study of the atmospheric pressure loading signal in VLBI observations, *J. geophys. Res.*, **109**(B03405), doi:10.1029/2003JB002500.
- Premoli, A. & Tavella, P., 1993. A Revisited three-cornered hat method for estimating frequency standard instability, *IEEE Trans. Instrument. Measure.*, **42**(1), 7–13.
- Ramillien, G., Frappart, F., Cazenave, A. & Güntner, A., 2005. Time variations of the land water storage from an inversion of 2 years of GRACE geoids, *Earth planet. Sci. Lett.*, **235**, 283–301.
- Ray, J., Altamimi, Z., Collilieux, X. & van Dam, T., 2008. Anomalous harmonics in the spectra of GPS position estimates, *GPS Solut.*, **12**(1), 55–64.
- Ray, J., 2011. Consistency of crustal loading signals derived from models and GPS. Inferences for GPS positioning errors, in *Proceedings of the AGU Fall Meeting 2011*, Session G51B-06, San Francisco, 9 December 2011.
- Rodell, M. et al., 2004. The Global Land Data Assimilation System, *Bull. Am. Meteorol. Soc.*, **85**(3), 381–394.
- Rodell, M., Chen, J., Kato, H., Famiglietti, J., Nigro, J. & Wilson, C., 2007. Estimating ground water storage changes in the Mississippi river basin using GRACE, *Hydrogeol. J.*, **15**, 159–166.

- Santamaria-Gomez, A., Bouin, M.-N., Collilieux, X. & Wöppelmann, G., 2011. Correlated errors in GPS position time series: implications for velocity estimates, *J. geophys. Res.*, **116**, B01405, doi:10.1029/2010JB007701.
- Schmidt, R., Flechtner, F., Meyer, U., Neumayer, K.H., Dahle, C., König, R. & Kusche, J., 2008. Hydrologic signals observed by the GRACE satellites, *Surv. Geophys.*, **29**(4–5), 319–334.
- Syed, T.H., Famiglietti, J.S., Rodell, M., Chen, J. & Wilson, C.R., 2008. Analysis of terrestrial water storage changes from GRACE and GLDAS, *Water Resour. Res.*, **44**, W02433, doi:10.1029/2006WR005779.
- Swenson, S. & Wahr, J., 2006. Post-processing removal of correlated errors in GRACE data, *Geophys. Res. Lett.*, **33**, L08402, doi:10.1029/2005GL025285.
- Swenson, S., Yeh, P.J.-F., Wahr, J. & Famiglietti, J., 2006. A comparison of terrestrial water storage variations from GRACE with in situ measurements from Illinois, *Geophys. Res. Lett.*, **33**, L16401, doi:10.1029/2006GL026962.
- Swenson, S.C., Chambers, D.P. & Wahr, J., 2008. Estimating geocenter variations from a combination of GRACE and ocean model output, *J. geophys. Res.-Solid Earth*, **113**(B8), B08410.
- Tapley, B.D., Bettadpur, S., Ries, J.C., Thompson, P.F. & Watkins, M.M., 2004. GRACE measurements of mass variability in the Earth system, *Science*, **305**(5683), 503–505.
- Tesmer, V., Steigenberger, P., van Dam, T. & Gürr, T.M., 2011. Vertical deformations from homogeneously processed GRACE and global GPS long-term series, *J. Geod.*, **85**, 291–310.
- Tregoning, P., Watson, C., Ramillien, G., McQueen, H. & Zhang, J., 2009. Detecting hydrologic deformation using GRACE and GPS, *Geophys. Res. Lett.*, **36**, L15401, doi:10.1029/2009GL038718.
- Tregoning, P. & Watson, C., 2009. Atmospheric effects and spurious signals in GPS analyses, *J. geophys. Res.*, **114**, B09403, doi:10.1029/2009JB006344.
- van Dam, T., Wahr, J. & Lavallée, D., 2007. A comparison of annual vertical crustal displacements from GPS and Gravity Recovery and Climate Experiment (GRACE) over Europe, *J. geophys. Res.*, **112**, B03404, doi:10.1029/2006JB004335.
- Wahr, J., Molenaar, M. & Bryan, F., 1998. Time variability of the Earth's gravity field: hydrological and oceanic effects and their possible detection using GRACE, *J. geophys. Res.*, **103**(B12), 30 205–30 229.
- Wahr, J., Swenson, S. & Velicogna, I., 2006. Accuracy of GRACE mass estimates, *Geophys. Res. Lett.*, **33**, L06401, doi:10.1029/2005GL025305.
- Watkins, M. & Yuan, D., 2007. JPL level-2 processing standards document for level-2 product release 04, GRACE 327–744 (Rev. 4.1).
- Zerbini, S., Richter, B., Rocca, F., van Dam, T. & Matonti, F., 2007. A combination of space and terrestrial geodetic techniques to monitor land subsidence: case study, the Southeastern Po Plain, Italy, *J. geophys. Res.*, **112**, B05401, doi:10.1029/2006JB004338.